ISSN 2176-5480

22nd International Congress of Mechanical Engineering (COBEM 2013)
November 3-7, 2013, Ribeirão Preto, SP, Brazil


# CHARACTERIZATION OF THE FLOW DYNAMICS IN THE EXPANSION CHAMBER OF A CYCLONIC SEPARATOR

**Hans E. Maldonado Ninahuanca**
**Henrique Stel**
LACIT/UTFPR, Av. Sete de Setembro 3165, Curitiba-PR-Brazil
hansmald@hotmail.com
stel.henrique@gmail.com

**Rigoberto E. M. Morales**
LACIT/UTFPR, Av. Sete de Setembro 3165, Curitiba-PR-Brazil
rmorales@utfpr.edu.br

***Abstract.*** *The present work presents a numerical study on the flow inside the expansion chamber of a hydrocyclone. This kind of flow is characterized by the development of a free-surface liquid film under the influence of both centrifugal and gravitational effects. The computational package ANSYS-CFX was employed to solve the problem. This program solves the momentum and mass conservation equations and provides a compressive model to deal with the interface. Numerical simulations for different input flow rates were carried out. Velocities and their axial and tangential components along streamlines were evaluated from the results of those simulations. The observed trends provided the basis for the development of an algebraic model for calculating the velocity field by approximating the streamlines to the pathline of a particle. The velocities' field modelling in this work can be used to help in the prediction of the flow dynamics inside a hydrocyclone, as well as in the design of an expansion chamber.*

***Keywords:*** *cyclonic separator, numerical simulation, velocity fields, streamlines.*

## 1. INTRODUCTION

Crude oil is usually associated with gas and reservoir water, the separation of this kind of mixture into their distinct phases at the wellhead is paramount to their transportation, through individual pipes, to a processing unit. This is done to prevent the occurrence of typical operational problems of multiphase flows: intermittent flows, hydrate formation, low centrifugal pump efficiency, deficient flow measurement of each individual phase and poor reservoir management.

The utilization of centrifugal force fields for separating liquid and gas is an emerging technique that presents some advantages when compared with the conventional gravity separation, namely: smaller (around 25%) processing unit areas, a 70%-85% reduction in the overall equipment load, greater separation efficiency with a fivefold reduction in separation times and ease of installation and operation (Nebrensky et al. 1980). Therefore, centrifugal separation became an economically attractive option for several operational scenarios, as it is the case of the offshore production, where load and space are critical factors.

Nowadays, cyclones are used in the design of several production systems. The present work focuses on the *Vertical Annular Separation and Pumping System* (VASPS) patented by United Kingdom's *British Petroleum* (BP) in 1988. This concept was designed for the offshore production of oil and gas and its operational specifics have been described and detailed by Gregory (1989).

Notwithstanding its compact design and ease of operation, the VASPS separator is not widely used in the petroleum industry, due to the problem posed by the accurate prediction of the flow dynamics inside the separator's expansion chamber. The combined action of both centrifugal and gravitational forces form a thin liquid film whose dynamics lack a reliable modeling, thus making it difficult to design new systems and improve existing ones given the operational conditions.

Levich (1962) published one of the earlier works on the flow of this thin liquid layer, seeking to describe the flow regimes as a function of the Reynolds number in the film. Malamatenios et al. (1994) demonstrated that the wall shear stress is the sole parameter involved in the balance of the gravitational forces acting on the film; he also showed that the liquid film thickness tends to a minimum which, once reached, remains constant. Rosa et al. (1996) carried out one of the first surveying studies on the influence of the centrifugal and gravitational field on a liquid film inside a cylindrical chamber and described the basic mechanisms governing the spatial distribution of those films. Morandin (1999) studied the behaviour of a liquid film under the combined action of the centrifugal and gravitational fields and came up with a mathematical model to predict the liquid flow behaviour. His model regards the flow as axisymmetric, a condition arising from the centrifugal forces tending to zero. However, the flow inside the separator is characterized by high speeds and strong variations in their components; therefore the solution presented by Morandin (1999) is a mere idealization of the actual phenomenon.

ISSN 2176-5480



Sant'anna (2010) carried out numerical simulations of flows in the expansion chamber. He figured out that the flow behaviour is dominated by the liquid flow rate, regardless of the presence of gas in the chamber. The numerical simulations were, therefore, similar in nature to those carried out for the single-phase flows. Ofuchi (2012) carried out a numerical study aimed to characterize the outflow of the expansion chamber.

Therefore, the behaviour of the liquid film in an expansion chamber is still an open subject that requires further investigation. A better understanding of the flow dynamics in a separator strongly depends upon studies on local liquid film velocities and inclination angles. The gist of the present work is to investigate the behaviour of the streamlines by calculating the velocities along a separator's expansion chamber. This goal was achieved by means of a numerical study based on computational fluid dynamics with the aid of the ANSYS-CFX package. A mathematical model aimed to predict the flow behaviour was developed and is henceforth presented.

## 2. DESCRIPTION OF THE PROBLEM

The objective of the present work is to analyze the liquid film velocity in an expansion chamber of a VASPS system's separator. A sketch of such device under normal operational conditions is shown in Figure 1. A separator's overall performance depends on the individual performance of each of its three main parts: the expansion chamber, the helix channel and the pool.

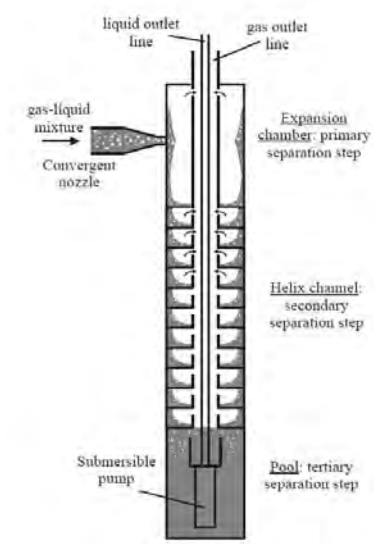


Figure 1. Schematics of the VASPS separation module

As Figure 2 illustrates, the liquid-gas mixture is accelerated in the nozzle, and enters the expansion chamber tangentially to its wall. Once inside the expansion chamber, the mixture flows along and close to the wall, forming a liquid film containing finely dispersed bubbles. The strong centrifugal field forces the bubbles to move along the radial direction in such a way that they may eventually reach the interface. Hence, as long as the liquid film flows, yet more gas separates from the mixture and joins the bulk of gas in the interior of the chamber. Most of the gas separation takes place in this chamber; experiments have determined that 70% of all the gas separates inside this region (Rosa et al. 2001). Therefore, a detailed study on the flow inside the expansion chamber becomes of pivotal importance.

ISSN 2176-5480



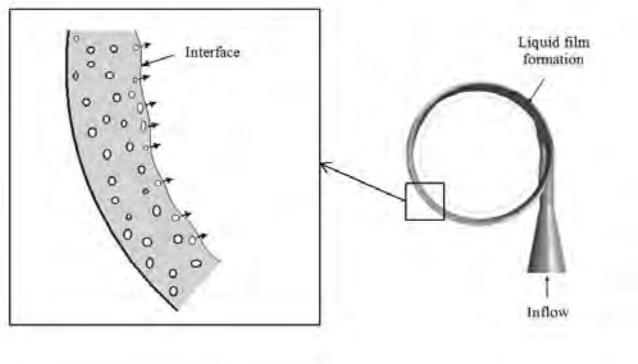


Figure 2. Liquid-gas separation in an expansion chamber

A better knowledge about the velocity fields within the liquid phase is essential to analyze the phase interaction and the liquid-gas separation, inasmuch as the flow field is dominated by the liquid flow rate, whether or not gas bubbles are present in the intake (Sant'anna, 2010). With all that in mind, the present work analyzes the single-phase flow at the separator intake, with the objective of studying the complex behaviour of the velocity field in the liquid phase.

## 3. MATHEMATICAL MODELLING

Figure 3 shows the flow of the liquid phase as it develops inside the expansion chamber under the influence of the centrifugal and gravitational force fields. Mass and balance conservation equations govern the behaviour of such flow. The present work considers single-phase flow at the inlet and the presence of free gas at the free surface condition. Therefore, the mathematical modeling uses a non-homogeneous approach based upon the two-fluid model.

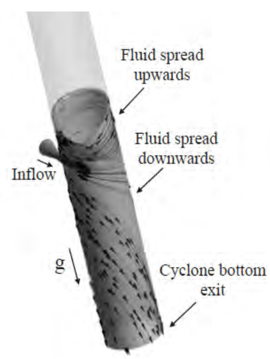


Figure 3. The flow dynamics inside the expansion chamber

### 3.1 Two-fluid model

The two-fluid model (Ishii [1975], Ishii and Mishima [1984]) is based on a stationary, Eulerian frame of reference and on averaged mass and momentum balances where the phases are treated as continuous and interpenetrating. This model is based on the following equations:

$$\frac{\partial \alpha_k \bar{\bar{\rho}}_k}{\partial t} + \nabla \cdot \left( \alpha_k \bar{\bar{\rho}}_k \hat{v}_k \right) = \Gamma_k \qquad (1)$$

$$\frac{\partial \alpha_k \bar{\bar{\rho}}_k \hat{v}_k}{\partial t} + \nabla \cdot \left( \alpha_k \bar{\bar{\rho}}_k \hat{v}_k \hat{v}_k \right) = -\nabla \left( \alpha_k \bar{\bar{p}}_k \right) + \nabla \cdot \left[ \alpha_k \left( \bar{\bar{\tau}}_k + \tau_k^T \right) \right] + \alpha_k \bar{\bar{\rho}}_k \hat{g}_k + M_k \qquad (2)$$

ISSN 2176-5480



where $k$ relates to a phase, $\alpha_k$ is the volumetric fraction of each phase, $\bar{\bar{\rho}}_k$ is the time-averaged phase density, $\hat{v}_k$ is the mass-averaged phase velocity, $\Gamma_k$ is the mass transfer, $M_k$ is the momentum transfer for each phase, $\bar{\bar{p}}_k$ is the pressure, $\hat{g}_k$ is the gravity, $\bar{\bar{\tau}}_k$ is the averaged stress due to viscous forces and $\tau_k^T = -\overline{\overline{\rho_k v_k^{'} v_k^{'}}}$ is the averaged stress due to turbulence.

There is no limitation for the number of phases this model can handle, but in general it is used for two phases only, that is, $k$=2. Also, the total sum of the volumetric fractions must be equal to unity:

$$\sum_{k=1}^{N} \alpha_k = 1 \tag{3}$$

The overall interface forces acting between two phases originate from several independent physical effects:

$$M_k = M^D + M^L + M^{LUB} + M^{VM} + M^{TD} + ... \tag{4}$$

The forces on the right hand side of Equation 4 above are, respectively, the drag, the lift, the wall lubrication, the virtual mass and the turbulent dispersion forces. In this work only the drag force is considered, all the others being disregarded due to their negligible influence on the development of the liquid film and for their limited scope (Ofuchi, 2002).

The drag force due to the contact between the two phases is modelled as:

$$M_{k=1}^D = C_D \rho_{12} A_{12} \left|\hat{v}_1 - \hat{v}_2\right| \left(\hat{v}_1 - \hat{v}_2\right) \tag{5}$$

where $C_D$ is the drag coefficient, $A_{12}$ is the interfacial area density per unit volume and $\rho_{12}$ is the specific mass of the mixture:

$$A_{12} = \left|\nabla \alpha_1\right| \tag{6}$$

$$\rho_{12} = \alpha_1 \rho_1 + \alpha_2 \rho_2 \tag{7}$$

The turbulent stress, $\tau_k^T$, is based on the turbulent viscosity and computed by the shear stress transport (SST), which combines the $k-\omega$ model for boundary layers with the $k-\varepsilon$ model for regions outside the said layer. A homogeneous modeling was assumed, in which the turbulence model equations are solved for a bulk field that comprises both phases, instead of separated equations for each phase.

### 3.2 Algebraic modelling

The present work proposes a computationally inexpensive method for solving the velocity field in an expansion chamber. The fundamental hypothesis behind the method for solving the velocities assumes that a small element of fluid could be approximated to the motion of a particle when subjected to the same gravitational and centrifugal field. The velocities for a particle at each point on the streamline are therefore obtained. The forces acting on a fluid element at any specific time are the wall forces, $F_w$, and the force due to its mass:

ISSN 2176-5480



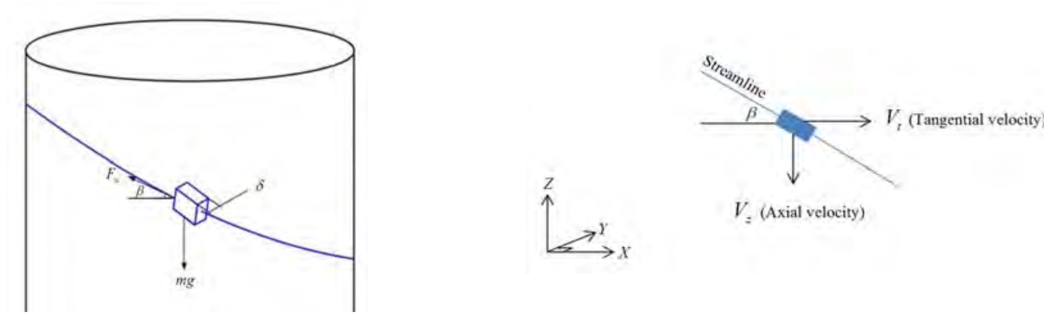


Figure 4. Forces acting on a particle inside the expansion chamber

Figure (4) shows how the velocity relationships expressed by Eq. (8) can be derived. $\beta$ is the angle formed by the streamline and the horizontal.

$$V = \frac{V_t}{\cos\beta} = \frac{-V_z}{\sin\beta} \tag{8}$$

The wall shear stress, given by Eq. (9) is derived from Darcy's Law and from Blasius' Power Law for Reynolds number, $\mathrm{Re}_\delta$, smaller than $10^5$ (Morandin 1999).

$$\tau_w = \frac{0.24}{8}\rho V^2 \,\mathrm{Re}_\delta^{-0.25} \tag{9}$$

The wall force, $F_w$, is the product of the wall shear stress by the contact area, $A$:

$$F_w = \tau_w A = \frac{0.24}{8}\rho V^2 \left(\frac{\rho V \delta}{\mu}\right)^{-0.25} A = \left(\frac{0.24}{8}\rho^{0.75}\mu^{0.25}A\right)V^{1.75}\delta^{-0.25} \tag{10}$$

Applying Newton's Second Law to the element depicted in Figure 4, yields:

$$m\frac{\partial}{\partial t}(V_t) = -F_w \cos\beta \tag{11}$$

$$m\frac{\partial}{\partial t}(V_z) = -mg + F_w sen\beta \tag{12}$$

Equations (13) and (14) are the equations of motion as proposed in the present work. They were derived from Eqs. (10), (11) and (12), considering two source terms, $\dot{\varphi}$, which represent the variations in velocity due to the interaction between a particle and its surroundings.

$$\frac{\partial}{\partial t}(V_t) = -\left[\left(\frac{0.24}{8}\rho^{0.75}\mu^{0.25}A\right)V^{1.75}\delta^{-0.25}\right]\frac{\cos\beta}{m} - \dot{\varphi}_t \tag{13}$$

$$\frac{\partial}{\partial t}(V_z) = -g + \left[\left(\frac{0.24}{8}\rho^{0.75}\mu^{0.25}A\right)V^{1.75}\delta^{-0.25}\right]\frac{sen\beta}{m} - \dot{\varphi}_z \tag{14}$$

The liquid film thickness is of pivotal importance in the development of the proposed model. This thickness is reached when the rule of the centrifugal forces on the flow inside the expansion chamber decrease and gravity forces

ISSN 2176-5480



become dominant. Should the length of the chamber be long enough the wall shear stress $\tau_w$ balances the gravitational force and from this point onwards both the liquid film thickness and velocity remain constant. This phenomenon is illustrated in Figure 5.

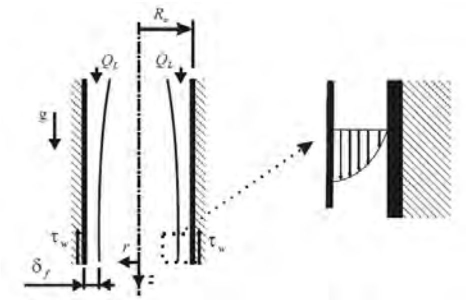

Figure 5. Scheme of the problem posed by a falling liquid film

The final values for the liquid film thickness, $\delta_f$, and the velocity $V_f$, for a turbulent regime are calculated by the following expressions (Morandin, 1999):

$$\delta_f = \left( \frac{0.24}{8} \left( \frac{Q_l}{2\pi R_0} \right)^{7/4} \frac{(\mu / \rho)^{0.25}}{g} \right)^{1/3} \tag{15}$$

$$V_f = Q_l / 2\pi R_0 \delta_f \tag{16}$$

where $Q_l$ is the flow rate at the inlet e $R_0$ the expansion chamber radius.

## 4. NUMERICAL MODELLING

In this section the two-fluid model equations will be discretized and solved with the Element-based Finite Volume Method (EbFVM) implemented in the software package ANSYS-CFX. The equations of the proposed model for the velocity field will be discretized as well.

### 4.1 The two-fluid model – discretization

The fluid is contained in a domain that comprises the inlet nozzle, and the cylindrical section of the expansion chamber, where the liquid film develops. The numerical grid/mesh for this domain is shown in Figure 6. The mesh is radially refined from the chamber walls onwards. That refinement is required as the liquid film is formed in this region. The refinement results in more accurate simulation results, and therefore a better determination of the gas-liquid interface. Another mesh refinement in the bordering region between the nozzle and the chamber, for that is a discontinuity zone in the chamber where the flow changes direction and undergoes a large variation in its velocity. After some tests, it was determined that a 600,000-element mesh is enough to achieve the simulations' goals.

ISSN 2176-5480



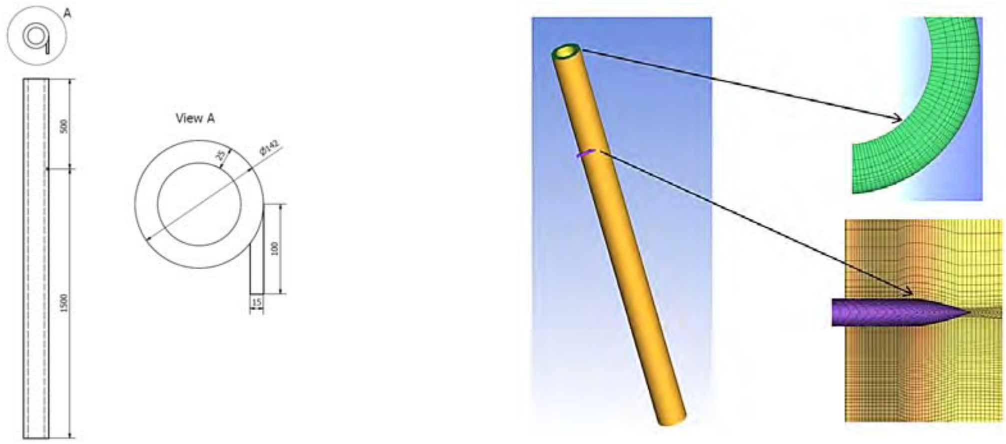


Figure 6. Geometry of the fluid domain under investigation and views of the numerical mesh

The EbFVM approach used in the simulations employs polyhedral control volumes around the vertexes of each of the elements of the mesh. Such a control volume is represented by the gray area shown in Figure 7.

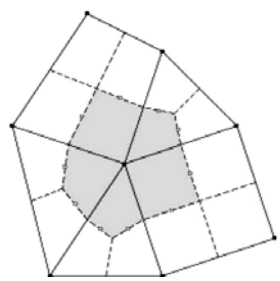

Figure 7. Element-based finite volume discretization of the spatial domain

The solid lines in Fig. 7 bound the limits of each element, whereas the dashed lines divide the elements into sectors. Variables are calculated at each black dot. Fluxes are evaluated at the hollow circles located between two neighbour control volumes. Integration point quantities, such as pressure and velocity gradients, are obtained from vertex values using finite element shape functions, except the volume fraction, which is obtained with a discretization based on the well-known Upwind scheme.

Conservation Equations (1) and (2) are then integrated over each control volume. The volume integrals are turned into surface integrals according to the Gauss divergence theorem. Time discretization is fully implicit.

In the following discussion, *V* is the volume of a control volume, $A_{ip}^{i}$ is the area of the face corresponding to an integration point, $\delta t$ is the time step and the superscripts $n + 1$ and $n$ indicate that a variable is evaluated at a new and an old integration time, respectively.

The discrete representation of the mass and momentum conservation equations are written as follows:

$$V\left[\left(\alpha_k\rho_k\right)_{cvc}^{n+1}-\left(\alpha_k\rho_k\right)_{cvc}^{n}\right]+\delta t\left[\sum_{ip}\left(\alpha_k\rho_k\hat{v}_k^i A^i\right)_{ip}^{n+1}\right]=0 \tag{17}$$

$$\begin{aligned}&V\left[\left(\alpha_k\rho_k\hat{v}_k^i\right)_{cvc}^{n+1}-\left(\alpha_k\rho_k\hat{v}_k^i\right)_{cvc}^{n}\right]+\delta t\left[\sum_{ip}\left(\alpha_k\rho_k\hat{v}_k^i\hat{v}_k^j A^j\right)_{ip}^{n+1}\right]=-\delta t\left[\sum_{ip}\left(\alpha_k p_k A^i\right)_{ip}^{n+1}\right]+\\&+\delta t\left[V\left(\alpha_k\rho_k g^i\right)\right]+\delta t\left[\sum_{ip}\left(\alpha_k\left(\overline{\overline{\tau}}_k^{ji}+\tau_k^{jiT}\right)A^j\right)_{ip}^{n+1}\right]+\delta t\left[V\left(M_k^i\right)\right]\end{aligned} \tag{18}$$

The discrete representation of Eq. (3) yields the equation for the volume continuity:

ISSN 2176-5480



$$\sum_{k=1}^{N} \alpha_k^{n+1} = 1 \tag{19}$$

The advection scheme used to evaluate the volume fraction, $\alpha_{k,ip}$, in terms of neighboring vertex is write in the form:

$$\alpha_{k,ip} = \alpha_{k,up} + \beta \nabla \alpha_k \cdot \vec{R} \tag{20}$$

where $\alpha_{k,up}$ is the upwind vertex value and $\vec{R}$ is the vector from the upwind vertex to the integration point and we introduce a compressive scheme by allowing $\beta > 1$.

The algebraic expressions in Eqs. (17), (18) and (19) are the equations for the volume fraction, velocity and pressure fields. For a two-phase system, these equations represent a coupled, 6x6 system of equations for each control volume and are solved simultaneously by means of a fully coupled algorithm. The supplementary transport equations, such as the one for turbulence, are not implicitly coupled to the system of equations for mass and momentum. The CFD package ANSYS-CFX was used to solve the set of equations presented in this section.

### 4.2 Solution of the algebraic model

This section presents the solution procedure of the proposed model and is explained the approach used to implement the source terms into the equations.

#### 4.2.1 Source terms

The purpose of the source terms included in the conservation equations is to represent the adjustments made in the dynamics of a particle so as to give it flow attributes. Figure 8 explains the nature of these terms. It shows three streamlines and P0 is the nozzle outlet. In this point, the three streamlines accelerate greatly in the axial direction due to the swift spread of the liquid over the wall. The streamlines intercept at points P1 e P2 thence transferring momentum in the process.

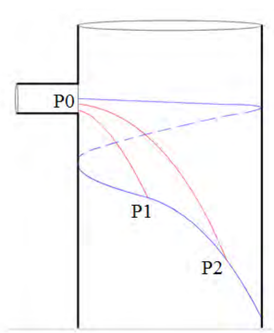


Figure 8. Streamlines in the expansion chamber and points where are implemented source terms

As per the previous discussion, it becomes clear that the source terms represent additional acceleration terms in the axial direction applied to the points P0, P1 e P2. Analyses of numerical simulations were required so as to obtain information about the strength of these source terms at three aforementioned points. Figure 9 presents the trend achieved for an inlet mass flow of 2 kg/s. As it can be observed, the acceleration at the nozzle (P0) is a few orders of magnitude above those accelerations arising from the intersection of the streamlines (P1 and P2).

ISSN 2176-5480



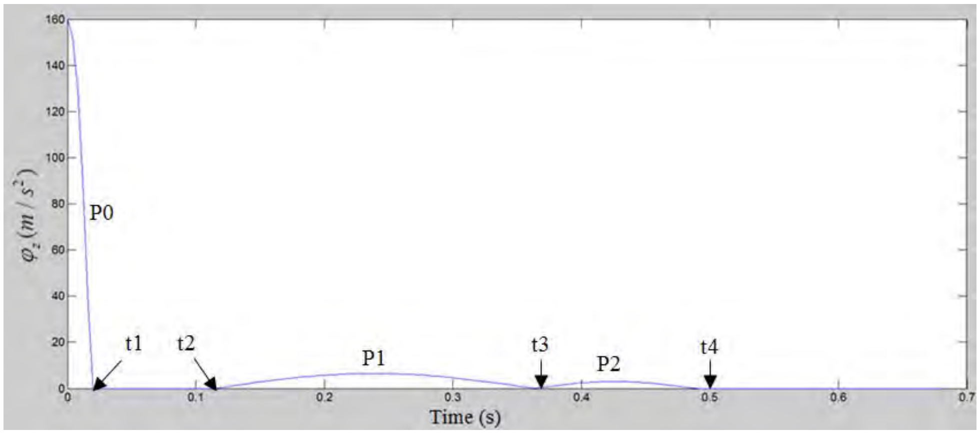


Figure 9. Source term axially oriented to the velocity (mass flow of 2 kg/s at the inlet)

As for the tangential direction, no source terms were included as it was found that in the selected test range (2-5 kg/s at the inlet) the initial equations properly describe the velocity in this direction. For the axial direction, the values obtained for the source terms are divided in discrete points and implemented at each timestep in the axial velocity component equation.

The liquid film thickness is assumed to vary linearly in the time interval [0 – $t1$], reducing its size from a value equal to the diameter of the nozzle to its final, constant size. After $t1$, the thickness remains constant throughout the expansion chamber.

$$\delta = \phi_b - t\frac{\left(\phi_b - \delta_f\right)}{t1} \qquad \left[0 - t1\right\rangle \tag{21}$$

$$\delta = \delta_f \qquad \left[t1 - t_f\right\rangle \tag{22}$$

$\delta$ is the film thickness as a function of time, $\delta_f$ is the final film thickness as per Eq. (15) and $\phi_b$ is the diameter of the nozzle.

#### 4.2.2 Solution of the system of equations of the algebraic model

The model's governing equations, Eqs. (13) and (14), describe a system of differential equations which was solved using Euler's integration method.

The calculation procedure requires the components of the initial velocity at the inlet of the separator. The tangential velocity at start up is approximated to the average velocity in the nozzle. The axial velocity at start up is zero as the nozzle directs the jet horizontally.

The variation of each component is computed from the initial velocities and therefore the velocity in the next time step is calculated by the following equations:

$$V_t^{n+1} = V_t^n + \left(\frac{\partial V_t}{\partial t}\right)_n \Delta t = V_t^n + \left(-\left[\left(\frac{0.24}{8}\rho^{0.75}\mu^{0.25}A\right)V^{1.75}\delta^{-0.25}\right]\frac{\cos\alpha}{m} - \dot{\varphi}_t\right)_n \Delta t \tag{23}$$

$$V_z^{n+1} = V_z^n + \left(\frac{\partial V_z}{\partial t}\right)_n \Delta t = V_z^n + \left(-g + \left[\left(\frac{0.24}{8}\rho^{0.75}\mu^{0.25}A\right)V^{1.75}\delta^{-0.25}\right]\frac{sen\alpha}{m} - \dot{\varphi}_z\right)_n \Delta t \tag{24}$$

where $n$ is the present time step and $n+1$ is the next one. The source term in the tangential direction is considered zero, $\dot{\varphi}_t = 0$ . The angle between the components of the velocities is kept updated time-wise:

ISSN 2176-5480



$$\alpha^{n+1} = \mathrm{arc}\,tg\left(\frac{-V_z^{n+1}}{V_t^{n+1}}\right) \tag{25}$$

The velocity field along a streamline from the nozzle to the outlet of the expansion chamber is obtained from Equations (23) and (24). With these results a tridimensional representation of a streamline can be obtained.

$$\theta^{n+1} = \theta^n + \frac{V_t}{R}\Delta t \tag{26}$$

$$X^{n+1} = R\cos(\theta^{n+1}) \tag{27}$$

$$Y^{n+1} = R\sin(\theta^{n+1}) \tag{28}$$

$$Z^{n+1} = Z^n + V_z\Delta t \tag{29}$$

where $\theta$ is the angular coordinate of the cylindrical expansion chamber, $R$ is its radius and $(X,Y,Z)$ are the coordinates of each point along the streamline.

## 5. RESULTS

### 5.1 Numerical simulations

Let the position $r$ be the vertical distance from the nozzle's centerline to the starting position of a streamline. Thus, to each velocity a correspondent streamline whose trajectory starts at $r$ can be drawn, see Figure 10.

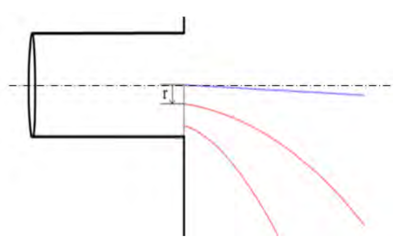


Figure 10. Definition of the position $r$ at the inlet

Figure 11 shows the results for the axial velocity. As shown, the velocity behaviour strongly depends upon the chosen streamline. Bigger initial accelerations correspond to distant $r$'s, whereas the opposite is observed as for the influence of the intersection of streamlines, that is, its strength decreases with increasing $r$. All velocities converge to a terminal value for points distant from the inlet, as suggested by Morandin (1999), see Equation (16). This equation predicts a terminal velocity of 2.31 m/s for the present case, therefore indicating that the numerical results and the theory developed by Morandin (1999) are consistent.

ISSN 2176-5480



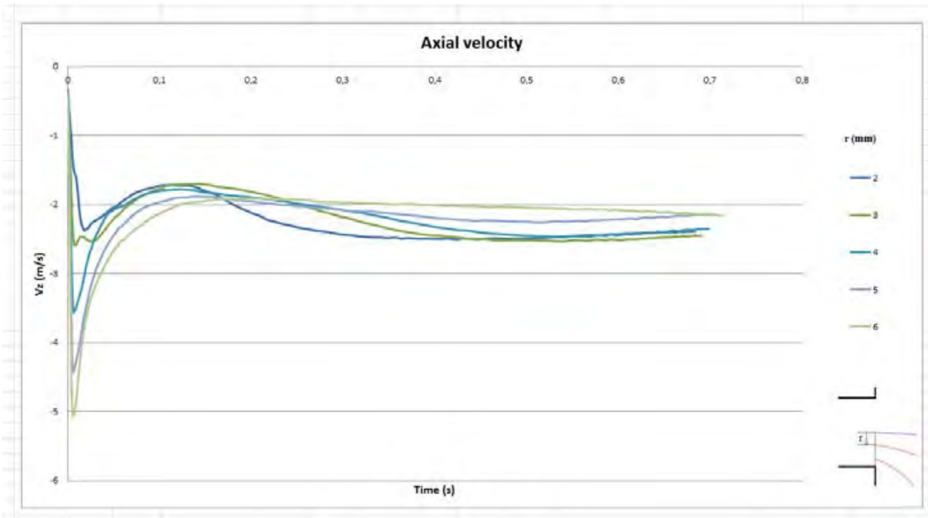


Figure 11. Axial velocity in function of time for selected streamlines (mass flow of 2 kg/s at the inlet)

Figure 12 shows the tangential velocity for a few streamlines. It was found that the behaviour of the velocity does not depend on the selected streamline, as all results show a common trend. Also, as it can be seen, the velocities drop rapidly within a quite narrow time interval. Such a time interval is rather important in the design of a separator, as its direct relationship to the centrifugal effects to phase separation plays a relevant role in the efficiency of the equipment. It should also be emphasized that regions far from the nozzle all tangential velocities tend to zero.

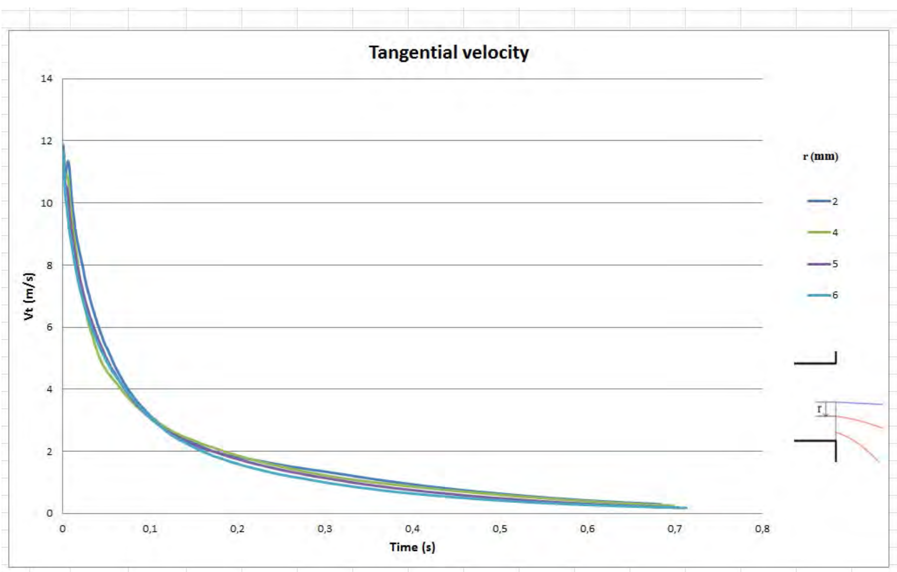


Figure 12. Tangential velocity as function of time for selected streamlines (inlet mass flow rate of 2 kg/s)

## 5.2 Algebraic model: results

The model herein developed describes the behaviour of the velocity along a streamline that goes from the nozzle to the lower part of the expansion chamber.

To compare the results of the proposed model with the numerical simulations, it was assumed a streamline close to the nozzle's centerline that would be free of numerical fluctuations. The results showed in this case is for $r$ = 2 mm.

The model was tested for flows in the 2 – 5 kg/s separator mass flow rate range at its inlet. Such is the range used by Morandin (1999) in its experimental expansion chamber and whose dimensions are close to the ones used in the present work.

ISSN 2176-5480



Figure 13 shows plots of results from the algebraic model and the numerical simulations so that they can be compared. The variation of the axial velocity in some specific regions can be explained on the grounds of the nature of the source terms, as these latter were implemented as pulses over short time intervals when they in fact are forces whose distribution spans over time. The fair trends shown by the tangential velocity curves dispensed the inclusion of additional source terms. However, a source term considering the flow spreading might have been included; that would help explaining the swift decrease in the velocity in regions nearby the inlet.

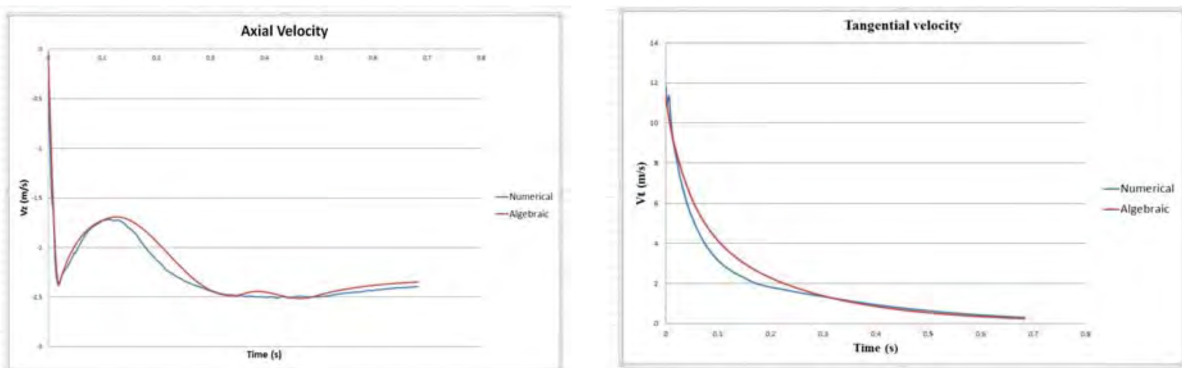


Figure 13. Axial and tangential velocities of the developed model (mass flow rate of 2 kg/s at the inlet)

Figure 14 shows the development of a streamline along the separator chamber. It was found out that in the proposed model the trajectory of the streamline shows an extra 0.5 spiral vis-à-vis the numerical simulation. This difference is due to the errors observed during the prediction of the velocity components.

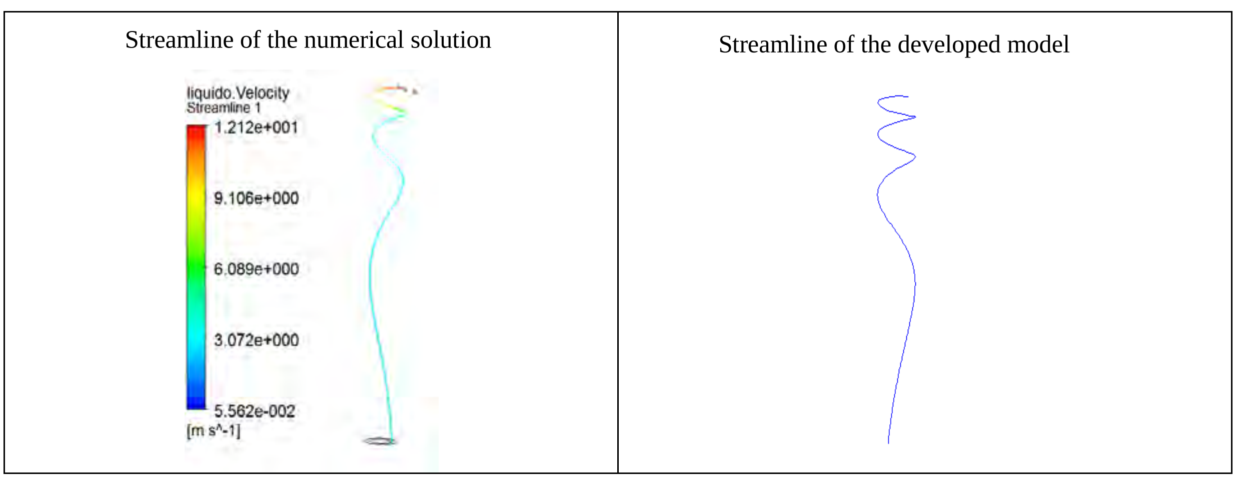


Figure 14. Streamline along the expansion chamber

Figure 15 shows the angles formed by the streamlines with the horizontal at each point along the streamline. As it can be observed, the angle increases very quickly in regions close to the nozzle to gradually and asymptotically tend towards a 90 degree angle.

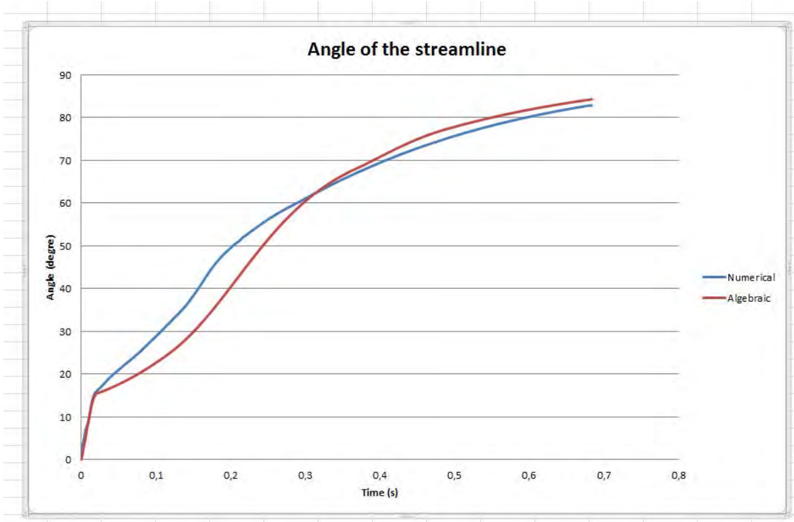


Figure 15. Angle of the streamline

The results obtained with the model proposed in this work agree well with the numerical simulations. The source terms provide a better comprehension of the phenomena and give a good estimation for the quantities evaluated in respect to the physics of the problem. The model is dependent of the source term values that result from the numerical simulations. The behavior of the source terms seems to follow a common trend for the whole range of flow rates considered, hence a deeper analysis of this behavior is an important task that is intended to be performed in order to derive a more independent and complete model. Also, it is expected that the tendencies here observed can be similarly applied for bigger separators by means of proper dimensional analysis.

## 6. CONCLUSIONS

A numerical study on the flow inside an expansion chamber of a cyclonic separator has been presented. The goal of the present work is to develop an algebraic model to predict the velocity field.

The results showed that the behaviour of the velocity in a streamline can be better described by means of an analysis of the movement of a particle. In order to obtain more accurate results, the equations of motion can be adjusted by the inclusion of a source term representing the interaction of a particle with its surroundings.

The formulation employed to calculate the shear stress on a wall showed results consistent to the physical principles involved in the problem. It was observed that the terminal velocity in the axial direction, according to the model, converges to the numerically calculated velocity.

The velocity components according to the proposed model were found to be in good agreement with the numerical simulations. Therefore, accurate results were obtained for the absolute velocity, the angle at each point of the streamline and the residence time of the fluid inside the expansion chamber. The error obtained from the number of turns of the streamline is explained by the rapid reduction of tangential velocity near the nozzle and better predictions can be obtained with the inclusion of a source term in this direction.

In general terms, the present work brings forth a fundamental work on the flow dynamics inside an expansion chamber. With the algebraic model herein presented, rather accurate predictions of the flow behaviour inside a chamber can be obtained, therefore dispensing with costly numerical simulations.

## 7. REFERENCES

ANSYS, 2011, *ANSYS - Solver Theory Guide*. ANSYS Inc., Canonsburg, PA, USA.

Ishii, M. and Hibiki, T., 2005. *Thermo-Fluid Dynamics of Two Phase Flow*. Eyrolles, France.

França, F.A., Rosa, E.S., Bannwart, A.C. and Moura, L.F., 1996. *Hydrodynamic studies on a cyclonic separator*. The Offshore Technology Conference, Houston, Texas, USA.

Gregory, J., 1989. *VASPS (Vertical Annular Separator and Pumping system) sends subsea separation on downward spiral to success*. Offshore Engineer, 24, pp. 35-36.

Levich, V.G., 1962. *Physiochemical Hydrodynamics*. New York, USA, Prentice-Hall, p. 669-692.

ISSN 2176-5480



Malamatenios, C., Glannakoglou, K.C., Papailiou, KD. 1994. *A coupled two phase shear layer/liquid film calculation method. Formulation of the physical problem and solution algorithm*. Int. J. Multphase Flow. Great Britain, v.20, n.3, p. 593-612.

Morandin, M.L., 1999. *Liquid film modeling under combined action fields of centrifugal and gravitational forces from: hydrocyclone (in Portuguese).* MS thesis, State University of Campinas, Campinas, SP, Brazil.

Nebrensky, N.T., Morgan, G.B., Oswald, B.J., 1980. *Cyclone for gas/oil separation*. Interational conference on hydrocyclone, Cambridge, England. p. 167-178.

Ofuchi, E.M., 2012. *Analysis of oil and gas flow in the expansion chamber of cyclonic separator VASPS (in Portuguese).* Final University Project, Federal Technological University of Paraná, Curitiba, Paraná, Brazil.

Rosa, E.S., Morandin, M.L., Dias, S.G. and França, F.A., 1996. *Liquid film motion under the action of gravitational and centrifugal fields.* ENCIT 96, Florianópolis, Brazil.

Rosa, E.S., França, F.A. and Ribeiro, G.S., 2001. *The cyclone gas–liquid separator: operation and mechanistic modeling.* Journal of Petroleum Science and Engineering, Rio de Janeiro, Brazil.

Sant'anna, F.O., 2010. *Numerical simulation of flow in expansion chamber gas-liquid separator VASPS.* Final University Project, Federal Technological University of Paraná, Curitiba, Paraná, Brazil.

Zwart, P.J., Godin, P.G., Penrose, J. and Rhee, S.H., 2008. *Simulation of unsteady free-surface flow around a ship hull using a fully coupled multi-phase flow method.* Journal of Marine Science and Technology, 13, pp. 346-355.